

Supporting Information

Oxygen defect engineering for Li-rich cathode material



Takashi Nakamura,^{*a} Kento Ohta,^b Xueyan Hou,^b Yuta Kimura,^a Kazuki Tsuruta,^c Yusuke Tamenori,^c Ryotaro Aso,^d Hideto Yoshida,^e and Koji Amezawa^a

^a Institute of Multidisciplinary Research for Advanced Materials, Tohoku University, 2-1-1 Katahira, Aoba-ku, Sendai, 980-8577 Japan

^b Graduate School of Engineering, Tohoku University, 6-6-1 Aramaki-Aoba, Aoba-ku, Sendai 980-8579, Japan

^c Japan Synchrotron Radiation Institute, 1-1-1, Kouto, Sayo-cho, Sayo-gun, Hyogo 679-5198, Japan.

^d Faculty of Engineering, Kyushu University, 744 Motooka, Nishi-ku, Fukuoka, 819-0395, Japan.

^e Institute of Scientific and Industrial Research, Osaka University, 8-1 Mihogaoka, Ibaraki, Osaka, 567-0047, Japan

Contents in the supporting information.

Supporting discussion 1. Site mixing in $\text{Li}_{1.2}\text{Ni}_{0.13}\text{Co}_{0.13}\text{Mn}_{0.54}\text{O}_{2-\delta}$.

Supporting discussion 2. Defect chemical analysis on the oxygen vacancy formation in $\text{Li}_{1.2}\text{Ni}_{0.13}\text{Co}_{0.13}\text{Mn}_{0.54}\text{O}_{2-\delta}$.

Supporting discussion 3. Thermodynamic analysis on the oxygen vacancy formation in $\text{Li}_{1.2}\text{Ni}_{0.13}\text{Co}_{0.13}\text{Mn}_{0.54}\text{O}_{2-\delta}$.

Figure S1. The oxygen vacancy formation of $\text{Li}_{1.2}\text{Ni}_{0.13}\text{Co}_{0.13}\text{Mn}_{0.54}\text{O}_{2-\delta}$ and $\text{Li}_{1.2}\text{Mn}_{0.6}\text{Ni}_{0.2}\text{O}_{2-\delta}$ [S5]. Calculated results of the defect equilibrium model (the equation S6) are shown by the dashed lines.

Figure S2. Partial molar enthalpy of oxygen of $\text{Li}_{1.2}\text{Ni}_{0.13}\text{Co}_{0.13}\text{Mn}_{0.54}\text{O}_{2-\delta}$ as a function δ .

Figure S3. SEM images of the (a) the pristine (oxygen-stoichiometric), (b) $\text{Li}_{1.2}\text{Ni}_{0.13}\text{Co}_{0.13}\text{Mn}_{0.54}\text{O}_{1.98}$ and (c) $\text{Li}_{1.2}\text{Ni}_{0.13}\text{Co}_{0.13}\text{Mn}_{0.54}\text{O}_{1.94}$.

Figure S4. XRD data and the calculated results of the Rietveld refinement for (a) the pristine (oxygen-stoichiometric), (b) $\text{Li}_{1.2}\text{Ni}_{0.13}\text{Co}_{0.13}\text{Mn}_{0.54}\text{O}_{1.98}$ and (c) $\text{Li}_{1.2}\text{Ni}_{0.13}\text{Co}_{0.13}\text{Mn}_{0.54}\text{O}_{1.94}$. R_{wp} and GOF were 11.70 and 1.91 for the pristine, 11.57 and 1.87 for $\text{Li}_{1.2}\text{Ni}_{0.13}\text{Co}_{0.13}\text{Mn}_{0.54}\text{O}_{1.98}$, and 10.95 and 1.78 for $\text{Li}_{1.2}\text{Ni}_{0.13}\text{Co}_{0.13}\text{Mn}_{0.54}\text{O}_{1.94}$.

Figure S5. Lattice parameters a , b , c and β , and the cell volume, V_{cell} , of $\text{Li}_{1.2}\text{Ni}_{0.13}\text{Co}_{0.13}\text{Mn}_{0.54}\text{O}_{2-\delta}$ ($C2/m$) as a function of δ .

Figure S6. Decomposition $P(\text{O}_2)$ of $\text{Li}_{1.2}\text{Ni}_{0.13}\text{Co}_{0.13}\text{Mn}_{0.54}\text{O}_{2-\delta}$ and $\text{Li}_{1.2}\text{Mn}_{0.6}\text{Ni}_{0.2}\text{O}_{2-\delta}$.

Figure S7. X-ray absorption spectra (a) at Ni L-edge of NiO (Ni^{2+}) and LiNiO_2 (Ni^{3+}) and (b) at Co L-edge of CoO (Co^{2+}) and LiCoO_2 (Co^{3+}).

Figure S8. X-ray absorption spectra of $\text{Li}_{1.2}\text{Ni}_{0.13}\text{Co}_{0.13}\text{Mn}_{0.54}\text{O}_{2-\delta}$ at (a) Ni-L, (b) Co-L and (c) Mn-L edge recorded by total electron yielding (TEY) method. Dashed lines are the spectra of the pristine (oxygen-stoichiometric) sample.

Figure S9. (a) The rate capability and cyclability, (b) the discharge capacity retention and (c) the energy density of $\text{Li}_{1.2}\text{Ni}_{0.13}\text{Co}_{0.13}\text{Mn}_{0.54}\text{O}_{2-\delta}$. The pristine sample was oxygen-stoichiometric.

Table S1. $I(003)/I(104)$ of $\text{Li}_{1.2}\text{Ni}_{0.13}\text{Co}_{0.13}\text{Mn}_{0.54}\text{O}_{2-\delta}$ assuming the $R\bar{3}m$ structure.

Table S2. Fitting parameters, $\Delta G_{\text{ox}}^{\circ}$ and a , of the equation S6, and the oxygen vacancy formation energy, $\Delta H_{\text{ox}}^{\circ}$, of $\text{Li}_{1.2}\text{Ni}_{0.13}\text{Co}_{0.13}\text{Mn}_{0.54}\text{O}_{2-\delta}$ and $\text{Li}_{1.2}\text{Mn}_{0.6}\text{Ni}_{0.2}\text{O}_{2-\delta}$.

Table S3. Average discharge capacity of $\text{Li}_{1.2}\text{Ni}_{0.13}\text{Co}_{0.13}\text{Mn}_{0.54}\text{O}_{2-\delta}$ as a function of the discharge rate.

Table S4. Total energy density of $\text{Li}_{1.2}\text{Ni}_{0.13}\text{Co}_{0.13}\text{Mn}_{0.54}\text{O}_{2-\delta}$ as a function of the cycle number.

Supporting discussion 1. Site mixing in $\text{Li}_{1.2}\text{Ni}_{0.13}\text{Co}_{0.13}\text{Mn}_{0.54}\text{O}_{2-\delta}$

The degree of the site mixing is evaluated from the ratio of the integrated peak intensity of 003 and 104 peaks in the $R\bar{3}m$ structure, $I(003)/I(104)$. $I(003)/I(104)$ is recognized as a suitable indicator of the degree of the cation mixing (the exchange of Li and TMs) [S1], $I(003)/I(104)$ of the pristine (the oxygen-stoichiometric) and the oxygen-deficient $\text{Li}_{1.2}\text{Ni}_{0.13}\text{Co}_{0.13}\text{Mn}_{0.54}\text{O}_{2-\delta}$ were calculated from their XRD patterns and summarized in **Table S1**. We found that 1) the intensity ratio is high suggesting the site mixing is negligibly small in our samples, and 2) the intensity ratio slightly decreased with increasing the oxygen vacancy concentration. These infer that the introduction of oxygen vacancy might enhance the cation mixing very weakly. For the simplicity, lithium at the transition metal site (Li^{TM}) and transition metal at the lithium site (TM^{Li}) were not considered in the Rietveld analysis in this work.

Table S1. $I(003)/I(104)$ of $\text{Li}_{1.2}\text{Ni}_{0.13}\text{Co}_{0.13}\text{Mn}_{0.54}\text{O}_{2-\delta}$ assuming the $R\bar{3}m$ structure.

| Sample | $I(003)/I(104)$ |
|--|-----------------|
| $\text{Li}_{1.2}\text{Ni}_{0.13}\text{Co}_{0.13}\text{Mn}_{0.54}\text{O}_2$ | 1.11 |
| $\text{Li}_{1.2}\text{Ni}_{0.13}\text{Co}_{0.13}\text{Mn}_{0.54}\text{O}_{1.98}$ | 1.08 |
| $\text{Li}_{1.2}\text{Ni}_{0.13}\text{Co}_{0.13}\text{Mn}_{0.54}\text{O}_{1.94}$ | 1.03 |

Supporting discussion 2. Defect chemical analysis on the oxygen vacancy formation in $\text{Li}_{1.2}\text{Ni}_{0.13}\text{Co}_{0.13}\text{Mn}_{0.54}\text{O}_{2-\delta}$

The formation of oxygen vacancy was studied based on defect chemistry. The equilibrium between oxygen gas and oxygen vacancy in the Li-rich phase is expressed by



The Gibbs free energy change of the equation S1, ΔG_{ox}° , is

$$\Delta G_{ox}^\circ = -RT \ln \left(\frac{[\text{V}_\text{o}^{\cdot\cdot}][\text{e}']^2 P(\text{O}_2)^{\frac{1}{2}} \gamma_{\text{V}_\text{o}^{\cdot\cdot}} \gamma_{\text{e}'}^2}{[\text{O}_\text{o}^\times] \gamma_{\text{O}_\text{o}^\times}} \right) - RT \ln \left(\frac{\gamma_{\text{V}_\text{o}^{\cdot\cdot}} \gamma_{\text{e}'}^2}{\gamma_{\text{O}_\text{o}^\times}} \right) \quad (\text{S2})$$

where, γ_i and $[i]$ are the activity coefficient and the molar concentration of i , respectively. The non-ideality in the system is considered as an excess-enthalpy, ΔH_{ex} , and the linear relation is assumed using the nonideal parameter, a , as applied in some nonstoichiometric oxides [S2-S5].

$$\Delta H_{ex} = RT \ln \left(\frac{\gamma_{\text{V}_\text{o}^{\cdot\cdot}} \gamma_{\text{e}'}^2}{\gamma_{\text{O}_\text{o}^\times}} \right) = a\delta \quad (\text{S3})$$

The conservation of the oxygen site and the charge neutrality are considered.

$$[\text{O}_\text{o}^\times] + [\text{V}_\text{o}^{\cdot\cdot}] = 2 \quad (\text{S4})$$

$$[\text{e}'] = 2[\text{V}_\text{o}^{\cdot\cdot}] \quad (\text{S5})$$

From equations S2-S5, the relation among δ - T - $P(\text{O}_2)$ is obtained.

$$P_{\text{O}_2}^{1/2} = \frac{2-\delta}{4\delta^3} \exp \left(-\frac{\Delta G_{ox}^\circ + a\delta}{RT} \right) \quad (\text{S6})$$

ΔG_{ox}° and a are the fitting parameters of the defect equilibrium model. This model is applied to $\text{Li}_{1.2}\text{Ni}_{0.13}\text{Co}_{0.13}\text{Mn}_{0.54}\text{O}_{2-\delta}$ and $\text{Li}_{1.2}\text{Mn}_{0.6}\text{Ni}_{0.2}\text{O}_2$ [S5]. The calculation results are shown in Figure S1 and the fitting parameters are summarized in Table S2. As shown in the figure, the defect equilibrium model can explain the initial stage of the oxygen vacancy formation in Li-rich cathodes. The oxygen vacancy formation energy, ΔH_{ox}° , is the enthalpy term of ΔG_{ox}° , and therefore, can be obtained from the temperature dependence of ΔG_{ox}° .

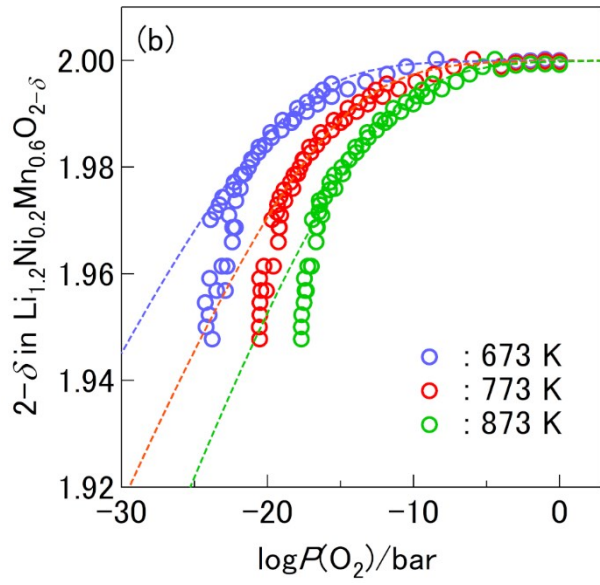
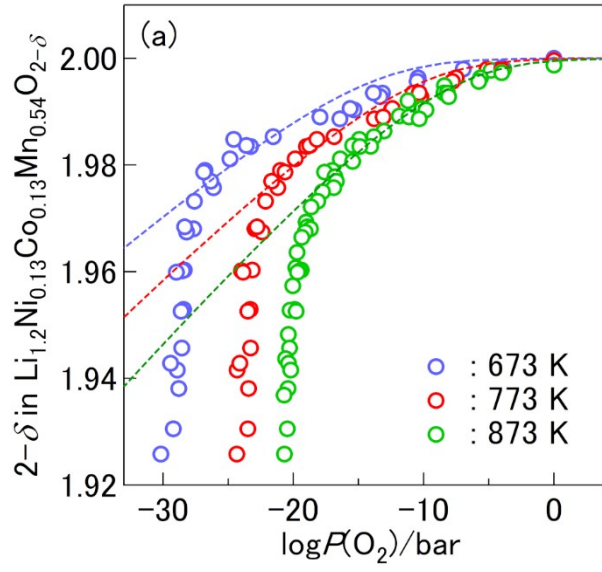


Figure S1. The oxygen vacancy formation of $\text{Li}_{1.2}\text{Ni}_{0.13}\text{Co}_{0.13}\text{Mn}_{0.54}\text{O}_{2-\delta}$ and $\text{Li}_{1.2}\text{Mn}_{0.6}\text{Ni}_{0.2}\text{O}_{2-\delta}$ [S5]. Calculated results of the defect equilibrium model (the equation S6) are shown by the dashed lines.

Table S2. Fitting parameters, ΔG_{ox}° and a , of the equation S6, and the oxygen vacancy formation energy, ΔH_{ox}° , of $\text{Li}_{1.2}\text{Ni}_{0.13}\text{Co}_{0.13}\text{Mn}_{0.54}\text{O}_{2-\delta}$ and $\text{Li}_{1.2}\text{Mn}_{0.6}\text{Ni}_{0.2}\text{O}_{2-\delta}$.

| | T/K | $\Delta G_{ox}^\circ/\text{kJ mol}^{-1}$ | $a/\text{kJ mol}^{-1}$ | $\Delta H_{ox}^\circ/\text{kJ mol}^{-1}$ |
|--|--------------|--|------------------------|--|
| $\text{Li}_{1.2}\text{Ni}_{0.13}\text{Co}_{0.13}\text{Mn}_{0.54}\text{O}_{2-\delta}$ | 673 | 165 | 2800 | 185 (1.92 eV) |
| | 773 | 162 | | |
| | 873 | 159 | | |
| $\text{Li}_{1.2}\text{Mn}_{0.6}\text{Ni}_{0.2}\text{O}_{2-\delta}$ | 673 | 183 | 1000 | 190 (1.97 eV) |
| | 773 | 182 | | |
| | 873 | 181 | | |

Supporting discussion 3. Thermodynamic analysis on the oxygen vacancy formation in $\text{Li}_{1.2}\text{Ni}_{0.13}\text{Co}_{0.13}\text{Mn}_{0.54}\text{O}_{2-\delta}$

The oxygen vacancy formation in $\text{Li}_{1.2}\text{Ni}_{0.13}\text{Co}_{0.13}\text{Mn}_{0.54}\text{O}_{2-\delta}$ was analyzed based on defect chemistry and thermodynamics. As the oxygen content was expressed by $2-\delta$, partial molar enthalpy of oxygen, $h_o - h_o^\circ$ can be calculated from the δ - T - $P(\text{O}_2)$ relationship by the following equation.

$$h_o - h_o^\circ = \frac{\partial}{\partial(1/T)} \left(\frac{R}{2} \ln P(\text{O}_2) \right) \quad (\text{S7})$$

$h_o - h_o^\circ$ can be considered as an indicator of the affinity of oxygen defects in the system. As summarized in **Figure S2**, $h_o - h_o^\circ$ decreases with δ until $\delta = 0.02$ and becomes almost constant in $0.02 < \delta < 0.06$. This suggests that the oxygen vacancy formation energy increases with δ in $0 < \delta < 0.02$, and such an excess energy is negligible in $0.02 < \delta < 0.06$. The cause of the excess energy for the defect formation is generally explained by defect interaction such as the defect associations, pairing, the defect-host interaction [S2, S3]. In these cases, the defect interactions usually increase with the defect concentration. This tendency is not consistent with $h_o - h_o^\circ$ of $\text{Li}_{1.2}\text{Ni}_{0.13}\text{Co}_{0.13}\text{Mn}_{0.54}\text{O}_{2-\delta}$. Figure S2 suggests that the major cause of the excess energy for the oxygen vacancy formation in $\text{Li}_{1.2}\text{Ni}_{0.13}\text{Co}_{0.13}\text{Mn}_{0.54}\text{O}_{2-\delta}$ is not typical defect interactions. The plausible explanation is the interaction of electronic structures and defect formation. Observed dependence of $h_o - h_o^\circ$ is consistent with the transition of the redox species, namely, strong interactions arise in Ni redox region ($0 < \delta < 0.02$) and defect interactions are negligible in Co redox region ($0.02 < \delta < 0.06$).

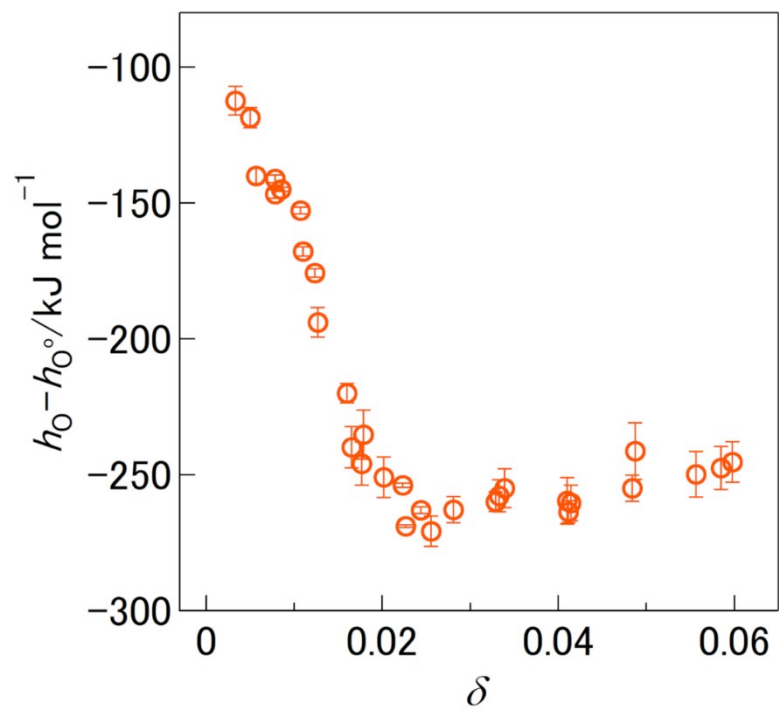


Figure S2. Partial molar enthalpy of oxygen of $\text{Li}_{1.2}\text{Ni}_{0.13}\text{Co}_{0.13}\text{Mn}_{0.54}\text{O}_{2-\delta}$ as a function δ .

Supporting references

- [S1] T. Ohzuku, A. Ueda, M. Nagayama, Electrochemistry and Structural Chemistry of LiNiO_2 (R3m) for 4 Volt Secondary Lithium Cells. *J. Electrochem. Soc.* **1993**, *140*, 1862.
- [S2] K. Yashiro, S. Onuma, A. Kaimai, Y. Nigara, T. Kawada, J. Mizusaki, K. Kawamura, T. Horita, H. Yokokawa, Mass Transport Properties of $\text{Ce}_{0.9}\text{Gd}_{0.1}\text{O}_{2-\delta}$ at the Surface and in the Bulk. *Solid State Ionics* **2002**, *152–153*, 469.
- [S3] S. Onuma, K. Yashiro, S. Miyoshi, A. Kaimai, H. Matsumoto, Y. Nigara, T. Kawada, J. Mizusaki, K. Kawamura, N. Sakai, H. Yokokawa, Oxygen Nonstoichiometry of the Perovskite-Type Oxide $\text{La}_{1-x}\text{Ca}_x\text{CrO}_{3-\delta}$ ($x=0.1, 0.2, 0.3$). *Solid State Ionics* **2004**, *174*, 287.
- [S4] T. Nakamura, K. Yashiro, K. Sato, J. Mizusaki, Oxygen nonstoichiometry and defect equilibrium in $\text{La}_{2-x}\text{Sr}_x\text{NiO}_{4+\delta}$. *Solid State Ionics* **2009**, *180*, 368.
- [S5] T. Nakamura, H. Gao, K. Ohta, Y. Kimura, Y. Tamenori, K. Nitta, T. Ina, M. Oishi, K. Amezawa, Defect Chemical Studies on Oxygen Release from the Li-Rich Cathode Material $\text{Li}_{1.2}\text{Mn}_{0.6}\text{Ni}_{0.2}\text{O}_{2-\delta}$. *J. Mater. Chem. A* **2019**, *7*, 5009.

Supporting figures

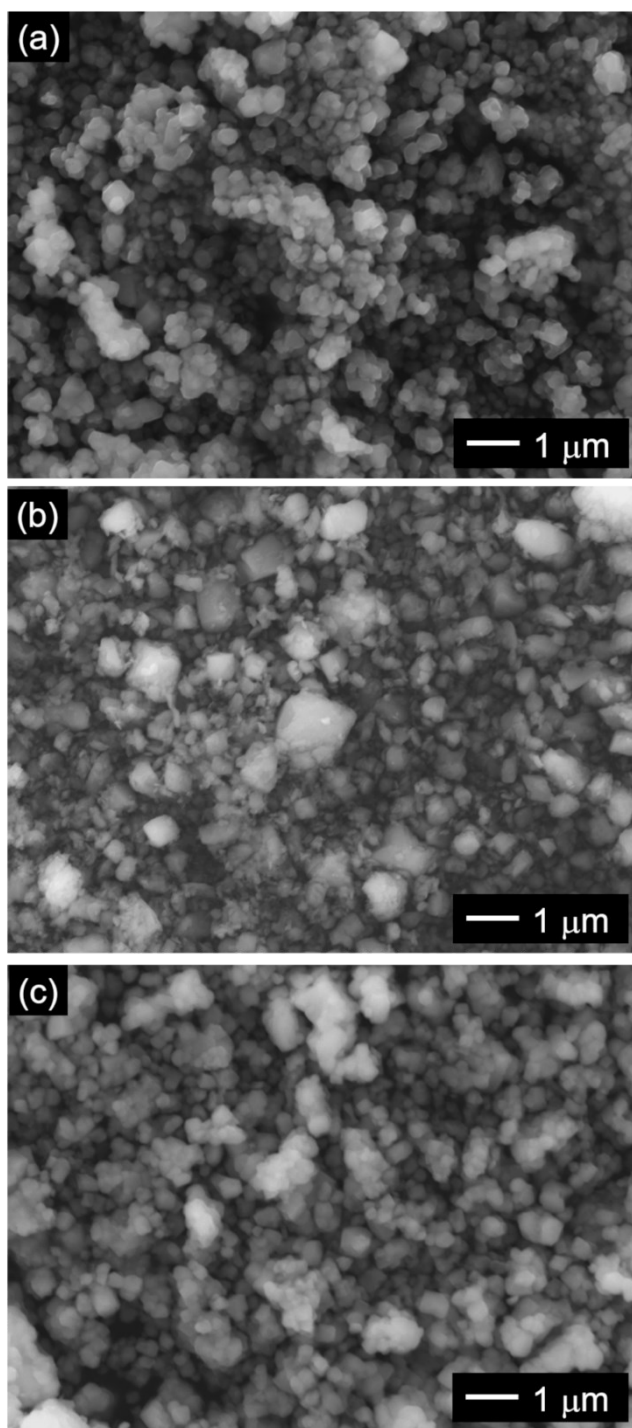


Figure S3. SEM images of the (a) the pristine (oxygen-stoichiometric), (b) $\text{Li}_{1.2}\text{Ni}_{0.13}\text{Co}_{0.13}\text{Mn}_{0.54}\text{O}_{1.98}$ and (c) $\text{Li}_{1.2}\text{Ni}_{0.13}\text{Co}_{0.13}\text{Mn}_{0.54}\text{O}_{1.94}$.

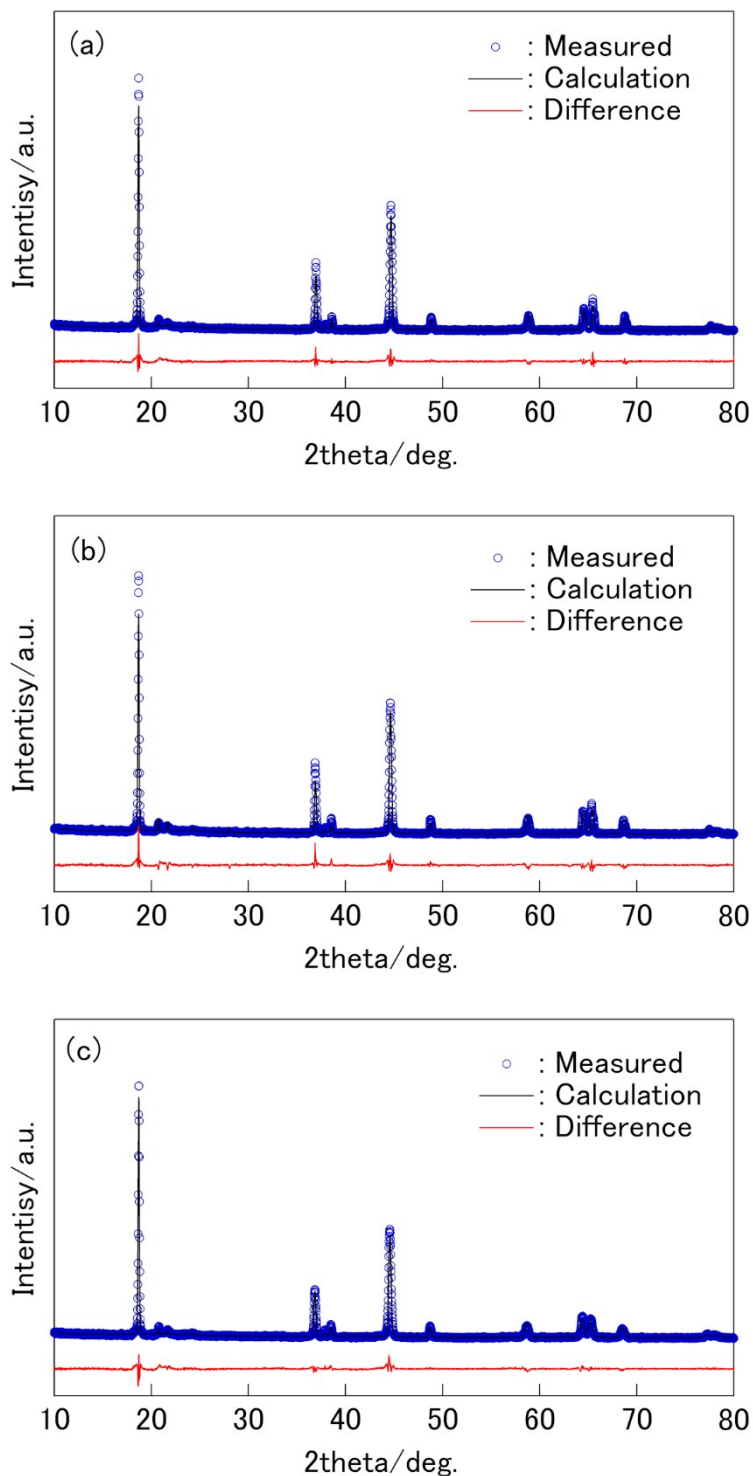


Figure S4. XRD data and the calculated results of the Rietveld refinement for (a) the pristine (oxygen-stoichiometric), (b) $\text{Li}_{1.2}\text{Ni}_{0.13}\text{Co}_{0.13}\text{Mn}_{0.54}\text{O}_{1.98}$ and (c) $\text{Li}_{1.2}\text{Ni}_{0.13}\text{Co}_{0.13}\text{Mn}_{0.54}\text{O}_{1.94}$. R_{wp} and GOF were 11.70 and 1.91 for the pristine, 11.57 and 1.87 for $\text{Li}_{1.2}\text{Ni}_{0.13}\text{Co}_{0.13}\text{Mn}_{0.54}\text{O}_{1.98}$, and 10.95 and 1.78 for $\text{Li}_{1.2}\text{Ni}_{0.13}\text{Co}_{0.13}\text{Mn}_{0.54}\text{O}_{1.94}$.

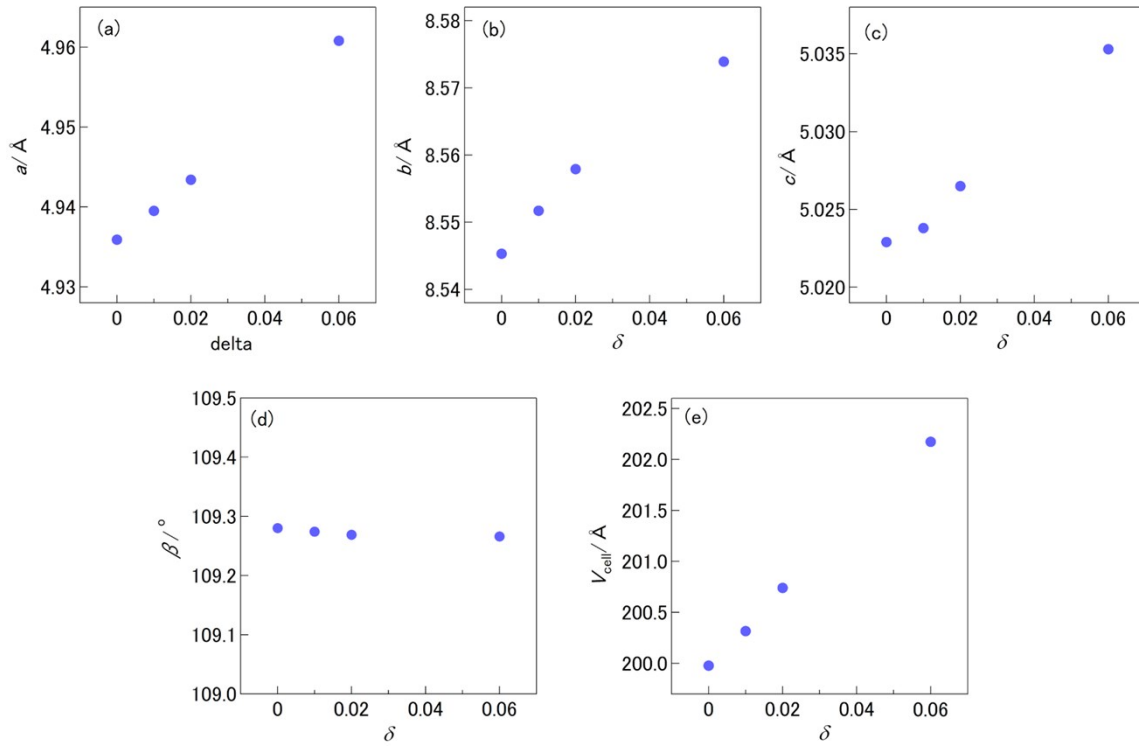


Figure S5. Lattice parameters a , b , c and β , and the cell volume, V_{cell} , of $\text{Li}_{1.2}\text{Ni}_{0.13}\text{Co}_{0.13}\text{Mn}_{0.54}\text{O}_{2-\delta}$ ($C2/m$) as a function of δ .

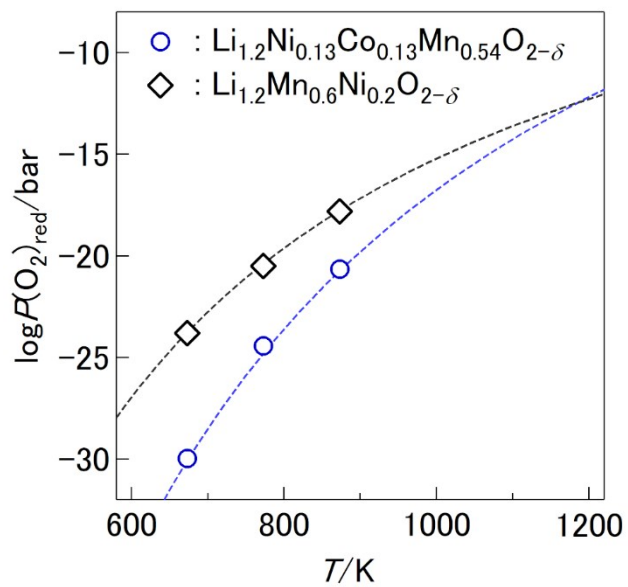


Figure S6. Decomposition $P(\text{O}_2)$ of $\text{Li}_{1.2}\text{Ni}_{0.13}\text{Co}_{0.13}\text{Mn}_{0.54}\text{O}_{2-\delta}$ and $\text{Li}_{1.2}\text{Mn}_{0.6}\text{Ni}_{0.2}\text{O}_{2-\delta}$ [S5].

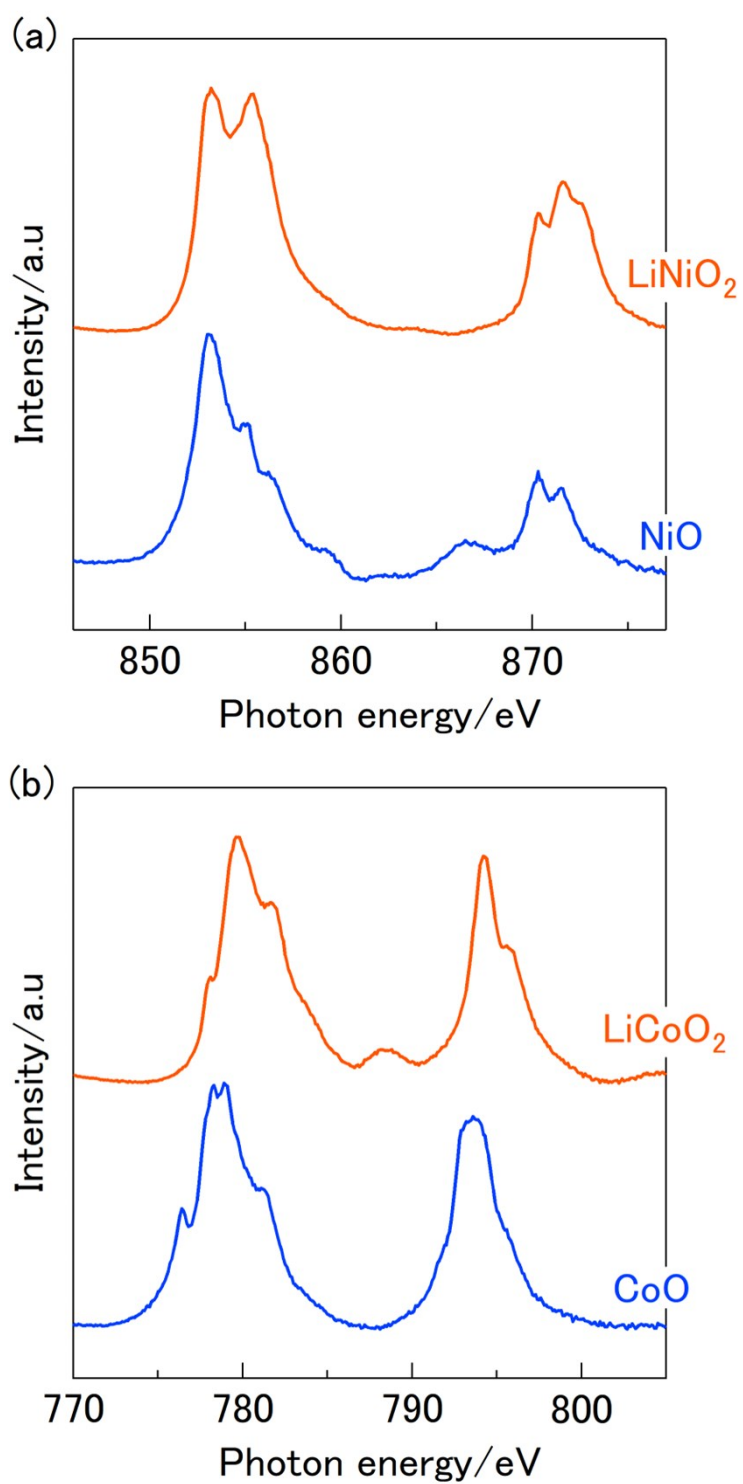


Figure S7. X-ray absorption spectra at (a) Ni L-edge of NiO (Ni^{2+}) and LiNiO_2 (Ni^{3+}), and (b) Co L-edge of CoO (Co^{2+}) and LiCoO_2 (Co^{3+}).

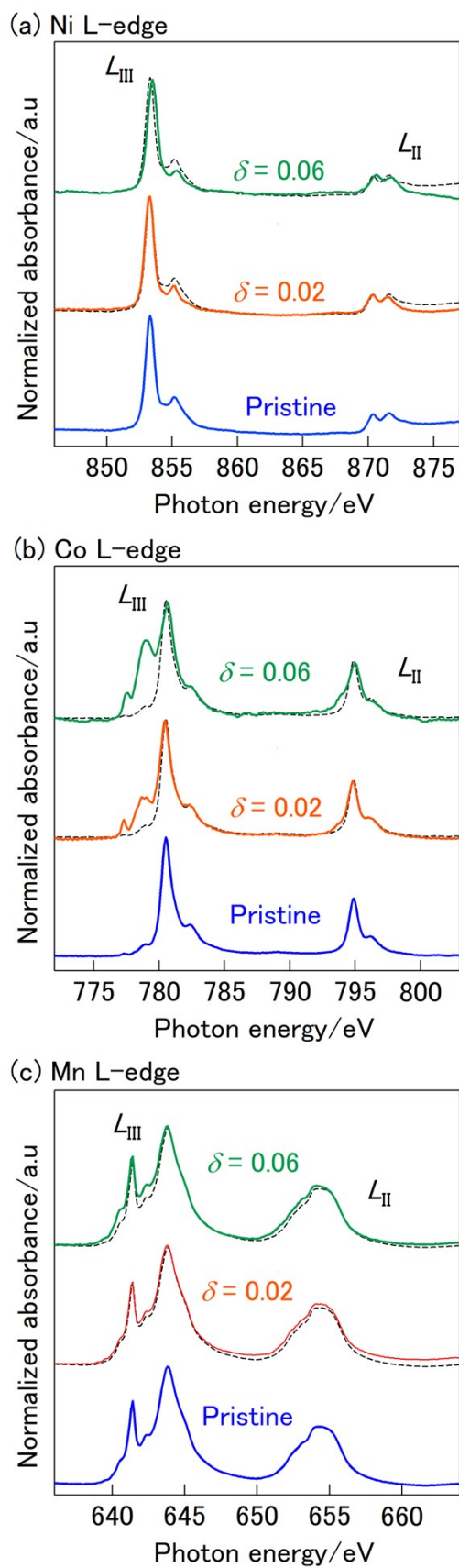


Figure S8. X-ray absorption spectra of $\text{Li}_{1.2}\text{Ni}_{0.13}\text{Co}_{0.13}\text{Mn}_{0.54}\text{O}_{2-\delta}$ at (a) Ni-L, (b) Co-L and (c) Mn-L edge recorded by total electron yielding (TEY) method. Dashed lines are the spectra of the pristine (oxygen-stoichiometric) sample.

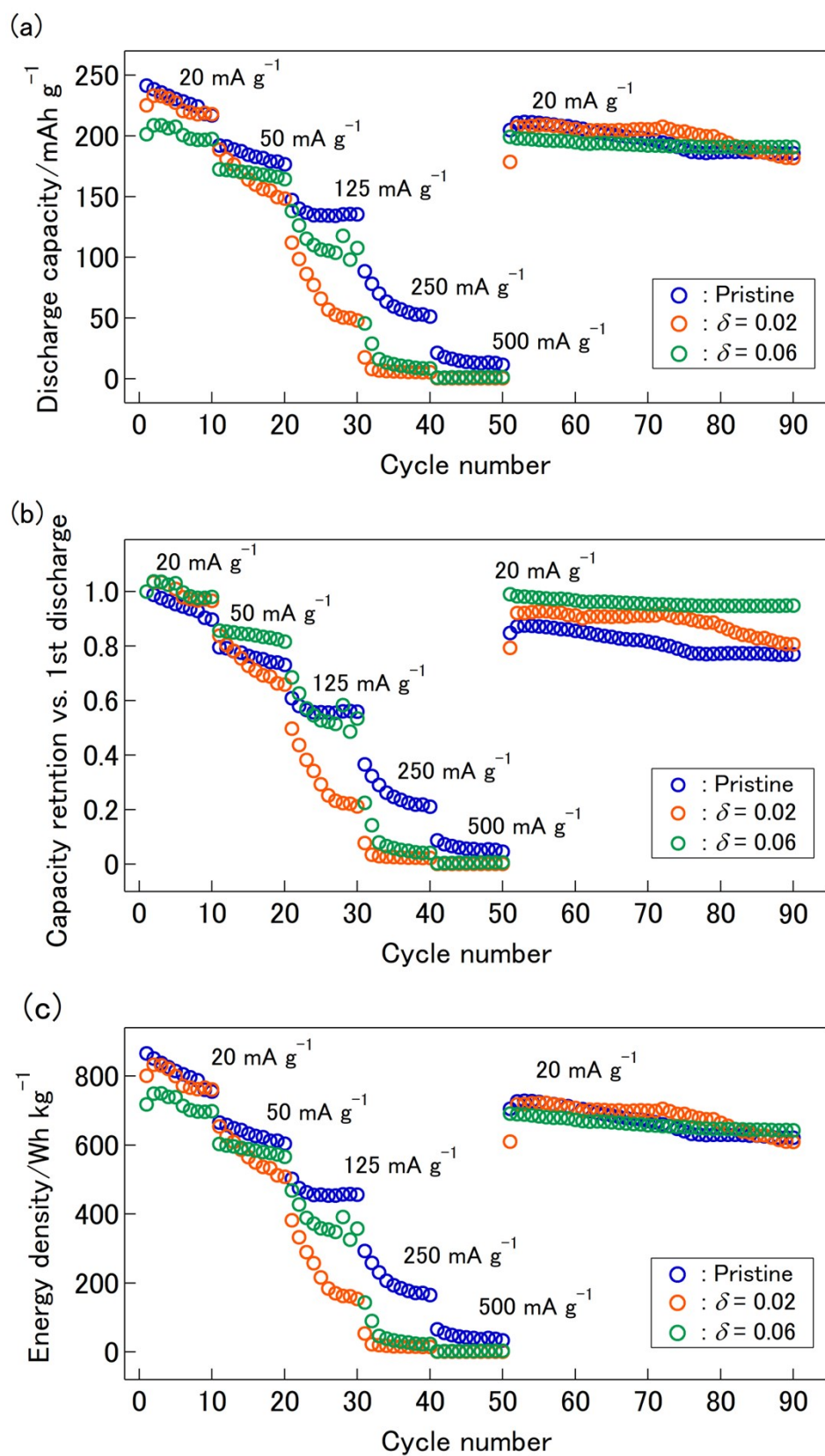


Figure S9. (a) The rate capability and cyclability, (b) the discharge capacity retention and (c) the energy density of $\text{Li}_{1.2}\text{Ni}_{0.13}\text{Co}_{0.13}\text{Mn}_{0.54}\text{O}_{2-\delta}$. The pristine sample was oxygen-stoichiometric.

Table S3. Average discharge capacity of $\text{Li}_{1.2}\text{Ni}_{0.13}\text{Co}_{0.13}\text{Mn}_{0.54}\text{O}_{2-\delta}$ as a function of the discharge rate.

| | $I = 20/\text{mA g}^{-1}$ | $I = 50/\text{mA g}^{-1}$ | $I = 125\text{mA g}^{-1}$ | $I = 250/\text{mA g}^{-1}$ |
|------------------------------------|---------------------------|---------------------------|---------------------------|----------------------------|
| Pristine ($\delta \approx 0$) | 229 mAh g ⁻¹ | 184 mAh g ⁻¹ | 137 mAh g ⁻¹ | 63.0 mAh g ⁻¹ |
| $\delta = 0.02$ | 224 mAh g ⁻¹ | 165 mAh g ⁻¹ | 69.8 mAh g ⁻¹ | 7.20 mAh g ⁻¹ |
| $\delta = 0.06$ | 202 mAh g ⁻¹ | 169 mAh g ⁻¹ | 113 mAh g ⁻¹ | 16.2 mAh g ⁻¹ |

Table S4. Total energy density of $\text{Li}_{1.2}\text{Ni}_{0.13}\text{Co}_{0.13}\text{Mn}_{0.54}\text{O}_{2-\delta}$ as a function of the cycle number.

| | 1 st /Wh kg ⁻¹ | 10 th /Wh kg ⁻¹ | 50 th /Wh kg ⁻¹ | 60 th /Wh kg ⁻¹ | 70 th /Wh kg ⁻¹ | 80 th /Wh kg ⁻¹ | 90 th /Wh kg ⁻¹ |
|------------------------------------|---|--|--|--|--|--|--|
| Pristine ($\delta \approx 0$) | 866 | 755 | 726 | 708 | 669 | 630 | 621 |
| $\delta = 0.02$ | 801 | 761 | 718 | 707 | 700 | 664 | 609 |
| $\delta = 0.06$ | 718 | 714 | 690 | 673 | 658 | 647 | 643 |